Electrochemical reduction of sulfite ions on a carbon ceramic electrode surface using prussian blue

[1]DR S ESWARA MURALI,[2]R.MOHANAPRIYA,[3] DR G NAGARAJAN,
[4]DR K SARITHA,[5]DR RAVURI SRINATH
Department of Pharmacology, Dr K.V Subba Reddy Institute of Pharmacy

ABSTRACT

Iodate, periodate, and sulphite ion detection using modified platinum electrodes with and without functionalized multi-walled carbon nanotubes (MWCNT-SO32-) and prussian blue nanoparticles (PB) is detailed in this paper. The modified electrodes were examined using tools including cyclic voltammetry (CVs), electrochemical impedance spectroscopy (EIS), electron dispersive X-ray spectroscopy (EDX), and transmission electron microscopy (TEM). When it came to electrocatalysis of iodate (IO3-), periodate (IO4-), and sulphite (SO32-), the Pt-MWCNT-PB electrode outperformed the others in terms of electron transport and catalytic efficiency. Some degree of adsorption owing to adsorbed intermediates was a defining feature of the electrode. Iodate had a Tafel value of 211.0 mVdec-1, periodate 176.2 mVdec-1, and sulphite 129.2 mVdec-1, indicating a high degree of adsorption. Micromolar levels of the analytes were observed. Iodate had a limit of detection of 8.30 μM (1.37x106 cm3mol-1s-1), periodate had an 8.06 μM (0.34x106 cm3mol-1s-1) value, and sulphite had a 4.70 μM (5.24 x 107 cm3mol-1s-1) value. Iodate may be detected by the electrode even when additional oxo-anions are present and interfering. You can trust this electrode to accurately measure iodate in both natural and synthetic salt solutions.

Keywords: iodate ion; periodate ion; sulphite ion; multi-walled carbon nanotubes; prusssian blue nanoparticles; modified electrode

1. INTRODUCTION

The identification and measurement of the oxoanions iodate (IO3−) and periodate (IO4−) in natural environments is highly desirable. For instance, iodate has a history of usage as an indicator in catalytic-kinetic studies involving redox reactions, despite reports that it is a hazardous ion [1]. The most common way that this ion might be exposed to in the environment is by drinking water [2]. During ozonization, iodide ions may transform into iodate, which is present in brackish water and, to a lesser degree, freshwater. The oxidant periodate, on the other hand, may oxidize a wide variety of inorganic and organic molecules at very low concentrations. The most effective method for preventing iodine or iodide deficient illnesses, including goitre, is to iodize table salt with potassium iodate or iodine, and this is done in most nations [3-5]. The food industry uses sulfites (SO32-) as a preservative to keep vitamin C and other foods from oxidizing [6]. Reduced oxygen concentrations, brought about by sulfites in natural water, may be harmful to aquatic life [7]. Sulfites are hazardous and may cause asthma attacks, mutations, and cancers [8,9]. It is crucial to ensure their removal from the environment and conversion to a less harmful form since these ions (IO4− and IO3−, SO32-) are poisonous, oxidizing, and carcinogenic.

Formula 4(III)[Fe(II)(CN)6]3 is the formula for prussian blue (PB), an iron cyanide complex. Biosensors [12], ion selective electrodes [10], charge storage devices [10], catalysis [11], and other areas have discovered uses for it as an electron-transfer mediator because of its outstanding electrocatalytic characteristics. The signal-to-noise ratio is enhanced with PB modified electrodes due to a dramatic reduction in background current. H2O2, glucose, hydrogen peroxide, and oxygen have all been detected using electrodes modified with carbon nanotubes and PB [13,14-16, 18–19]. Iodate and periodate [20-25] and sulphite (SO32-) [26,27] have been electrochemically detected on modified electrodes in recent publications. We are the first to know that an electrode modified with multi-walled carbon nanotubes/Prussian blue films on a platinum-based electrode would be used to detect these oxoanions. The second area of investigation concerned the redox properties of PB nanoparticles, namely their ability to oxidize sulphite and reduce iodate and periodate. Thirdly, the CNT-PB nanocomposite's electron transport characteristics as an electrode modification are little understood.

Chromatographic [28], spectrophotometric [29,30], and polarographic [31] techniques of ion measurement have all been used, but they all have their drawbacks, such the need for costly and complicated reagents and complicated experimental processes. Based on previous reports in the literature for a variety of compounds, an electrochemical method is simple, reproducible, and has lower limits of detection, making it a feasible way to detect these oxoanoins [22–27].

This research used PB nanoparticles to create an easy-to-use sensor for the electrocatalytic detection of sulphite, iodate, and periodate. The combination of MWCNTs and PB films on the Pt electrode was used to increase the electrochemical response to the analytes in a synergistic fashion. In comparison to other sensors described in the literature, this one had a low limit of detection, was simple to make, was electrochemically stable, reusable, and repeatable.

2. EXPERIMENTAL SECTION

2.1 Materials and Reagents

Multi-walled carbon nanotubes were purchased from Aldrich Chemical and were acid treated to introduce sulphonic functional group using a known procedure [32]. $FeCl_3$, $K_3[Fe(CN)_6]$, KCl, potassium iodate (KIO_3), potassium periodate (KIO_4) and sodium sulphite (Na_2SO_3) and other chemicals and reagent were of analytical grade and purchased from Sigma-Aldrich chemicals. Ultra-pure water of resistivity 18.2 MΩcm was obtained from a Milli-Q Water System (Millipore Corp., Bedford, MA, USA) and was used throughout the experiment. A phosphate buffer solution (PBS) of pH 2.0 was prepared with appropriate amounts of H_3PO_4 and $KH_2PO4.2H_2O$, and the pH was adjusted with 0.1 M H_3PO_4 or NaOH.

2.2. Equipment and Procedure

The energy dispersive x-ray spectra (EDX) were obtained from NORAN VANTAGE (USA). Transmission electron microscopy (TEM) characterisation was performed using a Tecnai G2 Spirit FEI (USA). Electrochemical experiments were carried out using an Autolab Potentiostat PGSTAT 302N (The Netherlands) driven by GPES and Frequency Response Analyser software. Electrochemical impedance spectroscopy (EIS) measurements were performed between 10 kHz and 0.1 Hz using a 5 mV rms sinusoidal modulation in 5 mM $[Fe(CN)_6]^{4-}/[Fe(CN)_6]^{3-}$ solution at a fixed dc potential of 0.2 V. The working, reference and counter electrodes used were Pt electrode, Ag|AgCl in saturated KCl and platinum wire respectively. A bench top BOECO pH meter, model BT-600 (Germany), was used for pH measurements. All solutions were de-aerated by bubbling argon for 10 minutes prior to each electrochemical experiment. All experiments were performed at 25 ± 1 °C.

2.3. Electrode modification procedure

Pt-MWCNT was prepared by a drop-dry method on a previously cleaned Pt electrode using 10 μL drop of the MWCNT solution (0.1 mg MWCNT in 1 mL DMF). The Pt-MWCNT electrode was dried in an oven at 50 °C for about 2 min. Electrodeposition of Prussian blue on the Pt-MWCNT and its activation was done by adopting a method earlier reported [33,34].

2.4. Determination of iodine content of iodated table salts

Three commercially available iodated table salts denoted as sample 1, 2 and 3 were analyzed for their iodine content. An accurately weighed (25 g) portion of a salt sample was transferred into a 100 mL beaker and dissolved by adding 80 mL pH 2.0 PBS. The clear solution was transferred to a 100 mL volumetric flask and made to mark with the PBS to give a stock solution of 250 g L^{-1}. 10 mL of this stock solution was pipette into each of 20 mL volumetric flask and all except one were spiked with different concentration of standard iodate solution (standard addition method), and made to volume with phosphate buffer pH 2.0. The current response of each test aliquot solution was determined using chronoamperometry. The experiment was repeated 5 times for each salt sample and average iodate content (in terms of iodine) obtained.

RESULTS AND DISCUSSION

3.1. Microscopic and spectroscopic characterisation

The TEM images of PB nanoparticles (Fig. 1a) and MWCNT-PB nanocomposite (Fig. 1b) show the formation of crystalline PB nanoplatelets on the Platinum (Pt) surface. Compared with PB alone, the MWCNT was interlocked between the nanoparticles as observed for MWCNT-PB probably due to strong π-π between the C=N groups of the PB and sp^2 hybridised carbon of the MWCNT. Ionic interaction between the two materials may be responsible for the maximum overlap observed (Fig. 1b). The average PB particle size distribution from the TEM image was estimated to be 18-30 nm. The reported particle sizes were obtained after calibrating the scale of the TEM image using the UTHSCSA Image Tool for windows version 3.0

The EDX profile (Fig. 1c) confirmed formation of PB nanoparticle due to the presence of the Fe peak. The hydrophilicity of the functionalised MWCNTs permits the movement and the adsorption of the free Fe^{3+} ions in solution to the interlayers of the MWCNTS. The reduced Fe^{3+}/Fe^{2+} ions during electrodeposition coordinated with the $[Fe(CN)_6]^{3-}$ anions forming PB . The prominent carbon peak could have been from the carbon of the MWCNTs and the cyanide (CN) group of the PB nanoparticles. The oxygen peak was attributed to the oxygen of the functionalised MWCNT- SO_3^{2-}.
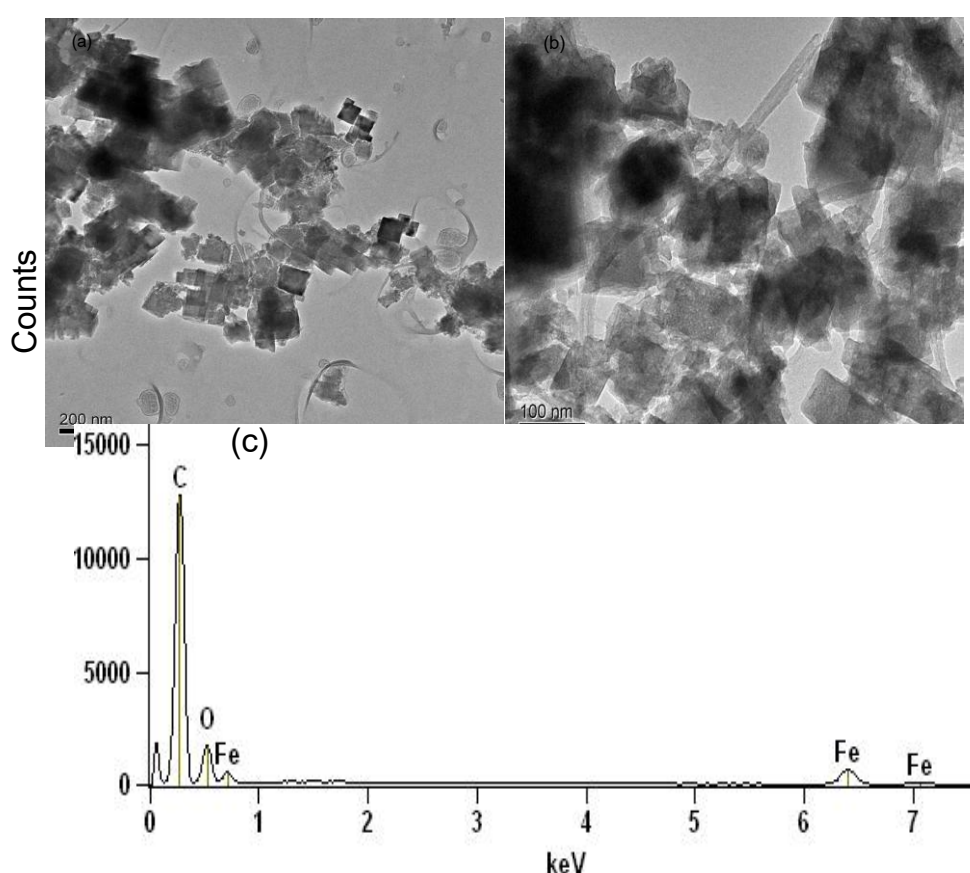
Figure 1. TEM of (a) PB nanoparticles, (b) MWCNT-PB nanocomposite (c) EDX profile of MWCNT-PB nanocomposite.

3.2. Electrochemical characterisation

Figure 2a compares the cyclic voltammograms of Pt-PB, and the Pt-MWCNT-PB in 0.1 M KCl electrolyte. One of the objectives of this work was to determine an enhanced electron transfer properties (in terms of current response) of the modified electrode as observed in Figure 2a. The presence of functionalised MWCNT resulted in the enhancement (five times) of PB redox currents on the Pt-MWCNT-PB electrode (9.68×10^{-2} mA) over Pt-PB modified electrode (1.79×10^{-2} mA) alone. Applying MWCNTs increases the surface area of the electrode, therefore contributing to increase in the surface coverage of PB, and consequently an increase in the PB redox current is observed. The result agreed with the recent report where introduction of MWCNT enhance the peak current of chitosan Prussian blue hollow platinum cobalt composite gold modified electrode (Cs-PB-MWNTs-H-PtCo/Au) compared with the current of Cs-PB-H-PtCo/Au electrode [33]. The redox couple on both electrodes was attributed to Prussian blue attaining its reduced form (Prussian white (PW)) as represented by equation 1 [35,36]:

$$KFe(III)[Fe(II)(CN)_6] + e^- + K^+ \longrightarrow K_2Fe(II)[Fe(II)(CN)_6] \quad (1)$$
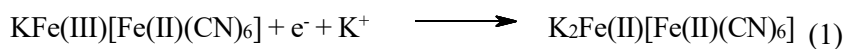
$$PB \qquad\qquad\qquad\qquad PW$$

The number of cycles or times of deposition plays a major part in ascertaining the amount and the current response of PB nanoplatelets deposited on the electrode [15,34]. Therefore, preliminary experiments in this study showed that 300s of deposition gave better redox current response which tends to be stabilised with increasing time. Assuming a transfer of four electrons per unit PB cell [37], the surface concentration of the redox species on the Pt-MWCNT-PB platform (Γ_{PB} / mol cm^{-2}) can be estimated from the area under the peak [38] using equations 2:

$$\Gamma_{PB} = \frac{Q}{nFA} \quad\qquad (2)$$

where Q is the area of the peak, A is the area of the electrode, F is the Faraday constant, and n is the number of electrons transferred. The value of the Γ_{PB} was estimated to be $\sim 3.2 \times 10^{-8}$ mol cm^{-2}. The value is greater than the 10^{-9}-10^{-10} mol cm^{-2} magnitude expected for a monolayer assembly [39], therefore, confirming the crystalline and aggregate form of the PB nanoparticles, which would have resulted from several layer of PB films as shown by the TEM image (Fig. 1). Figure 2b shows that the Pt-MWCNT-PB modified electrode possesses excellent electrochemical stability with no significant loss (*ca* 5%) in current and no shift in peak anodic and cathodic potentials even after repetitive cycling (30 cycles) in the electrolyte.

Meanwhile, cyclic voltammogram (CV) was also employed to compare the electron transfer behaviour and current responses of the different modified electrodes in 5 mM $[Fe(CN)_6]^{4-}$ / $[Fe(CN)_6]^{3-}$ redox probe (Fig. 3a). The CVs show the $[Fe(CN)_6]^{4-}$ / $[Fe(CN)_6]^{3-}$ redox peak at $E_{1/2}$ of *ca* 0.2 V which

was common to all the electrodes but with more pronounced current on Pt-MWCNT-PB (curve iv) which was due to the redox process of Prussian blue (PB) to Prussian white (PW).
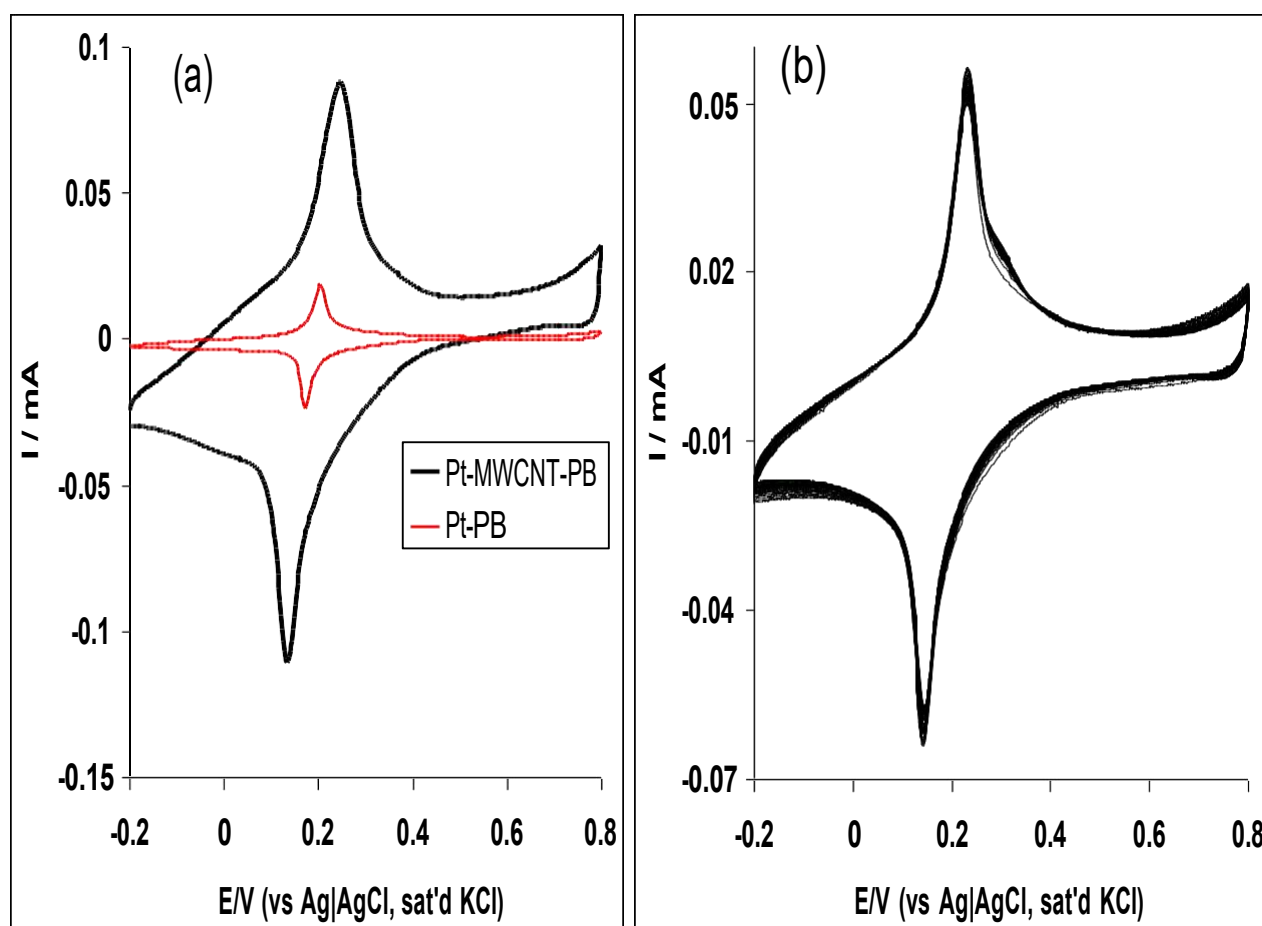

Figure 2. (a) Comparative cyclic voltammograms showing the current responses of Pt-PB and Pt-MWCNT-PB modified electrodes in 0.1 M KCl electrolyte (scan rate: 50 mVs^{-1}). (b) Repetitive cyclic voltammograms (30 cycles) of the Pt-MWCNT-PB modified electrode in 0.1 M KCl electrolyte.

Even though the Pt-MWCNT-PB showed redox peak at 0.2 V, similar to where the redox process of $[Fe(CN)_6]^{4-}$ / $[Fe(CN)_6]^{3-}$ occurs, however, the following attributes confirm the successful

modification of the Pt-MWCNT-PB electrode with PB nanoparticles. (1) compared with the bare Pt electrode with absence of PB particles (curve i), the enhanced oxidation and reduction current on the Pt-MWCNT-PB electrode (curve iv) was attributed to the heterogenous fast electron kinetics made possible by the functionalised MWCNT mediating between the base electrode (Pt) and the surface modifier (PB), (2) the second anodic peak at around 0.8 V, found on Pt-PB (curve iii) and Pt-MWCNT-PB (curve iv) but not found on the bare Pt electrode, was due to the formation of Prussian yellow (PY), an intermediate during PB oxidation [35,36], which further confirms successful modification of the electrodes with PB nanoparticles. Lastly, the cyclic voltammograms of the Pt-PB and Pt-MWCNT-PB electrodes in KCl electrolyte (i.e. in the absence of $[Fe(CN)_6]^{4-}$ / $[Fe(CN)_6]^{3-}$),

showed both redox peaks at around 0.2 V and 0.8 V attributed to PB nanoparticles. These peaks were absent on the bare Pt electrode in the same KCl electrolyte. The result obtained in this study can be likened to similar study where electrochemical and the electron transport properties of PB and Fe complexes modified electrodes were reported in probes such as $K_3Fe(CN)_6$ or $[Fe(CN)_6]^{4-}$ / $[Fe(CN)_6]^{3-}$ [33,41,42]

Further insight into the interface properties of the surface-modified electrode was probed using Electrochemical impedance spectroscopy (EIS) at a fixed potential (0.2 V vs. Ag|AgCl, sat'd KCl). The Nyquist plot obtained (Fig. 3b) confirmed many electrode/electrolyte interface processes. The linear part of the Nyquist plot represents the diffusion-limited process, while the semicircle portion corresponds to the electron transfer limited process. As clearly seen, the semicircle or the arc was very pronounced for the bare Pt (i) and Pt-PB (ii) modified electrode signifying high electron or charge transfer resistance of these electrodes compared with Pt-MWCNT (iii) or Pt-MWCNT-PB (iv) characterized with fast electron transfer kinetics. The impedance spectra obtained from this study were satisfactory fitted based on the % error and chi-square values using Randles equivalent circuit represented in Figure 4a, and the data obtained are presented in Table 1.0. R_s is the solution/electrolyte resistance, R_{ct} represents the charge-transfer resistance, C_{dl} or C_{film} represents true capacitance while Z_w represents the Warburg diffusion. Aside from visual inspection of goodness of the fitting lines, two accurate ways to establish how well the modeling functions reproduce the experimental data sets are the relative error estimates (in %) and chi-square functions (χ^2), which is the sum of squares of the relative residuals (i.e., sum of the real and imaginary χ^2), easily obtained from the K-K test. From Table 1.0, Pt-MWCNT-Pt has the lowest R_{ct} value (2.66 Ωcm^2) implying fastest electron transfer properties compared with the other electrodes investigated. Bode plot of –phase angle vs log f, (Fig. 4b), gave phase angles of 64.1^0 for Pt (i), 58.3^0 for Pt-PB (ii), 11.7^0 for Pt-MWCNT and 9.2^0 for Pt-MWCNT-PB (iv) which are less than the 90° expected of an ideal capacitive behaviour confirming the pseudocapacitive nature of these electrodes. However, since phase angle (ϕ) and the frequency at maximum phase angle ($f\phi$) are directly and inversely proportional to R_{ct} respectively [42,43], therefore, the lowest phase angle recorded for Pt-MWCNT-PB electrode in this study makes it the best electrode in terms of electron transport compared to the other electrodes.
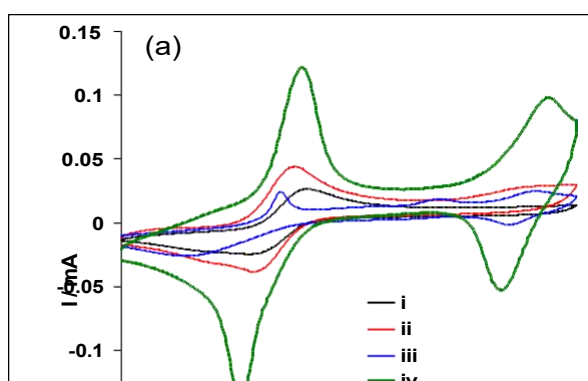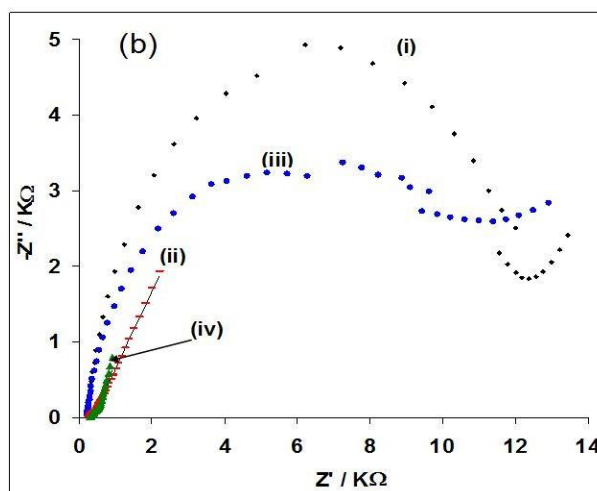
Figure 3. (a) Comparative current response of (i) Pt, (ii) Pt-MWCNT, (iii) Pt-PB and (iv) Pt-MWCNT-PB modified electrodes in 5 mM $[Fe(CN)_6]^{4-}/[Fe(CN)_6]^{3-}$ solution (pH 7.0 PBS). Scan rate = 50 mVs^{-1}. (b) Typical Nyquist plots of (i) Pt, (ii) Pt-PB, (iii) Pt-MWCNT and (iv) Pt-MWCNT-PB modified electrodes in 5 mM $[Fe(CN)_6]^{4-}/[Fe(CN)_6]^{3-}$ solution($E_{1/2} = 0.2$V).
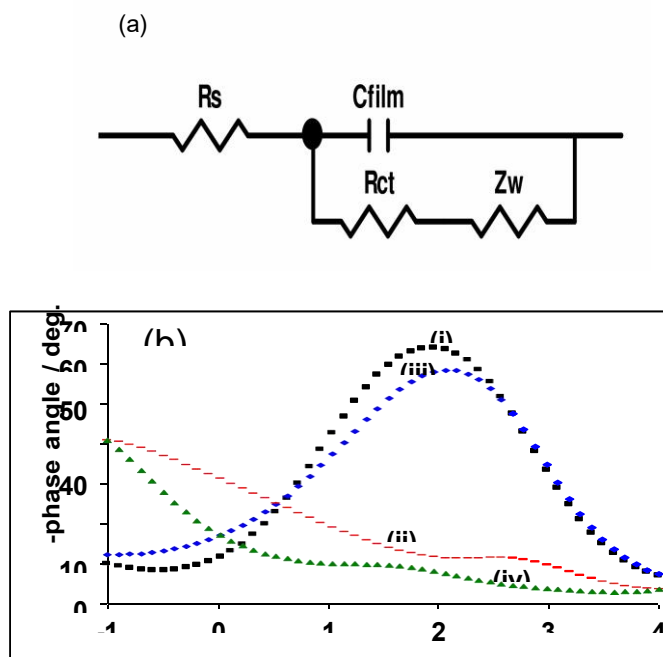
Figure 4. (a) Circuit diagram used in the fitting of the impedance data in Figure 3a. (b) Bode plots of – phase angle/deg. vs. log (f/Hz) for the electrodes in Figure 3b.

Table 1. Impedance data obtained for the Pt modified electrodes in 5 mM $Fe(CN)_6]^{4-}/[Fe(CN)_6]^{3-}$ solution at 0.2 V (vs Ag|AgCl sat'd KCl). All values were obtained from the fitted impedance spectra after several iterations using of the circuit. The values in parentheses are percentage errors of data fitting.

Electrode	Impedance Data				
	R_s /Ωcm^2	C_{film}/ μFcm^{-2}	R_{ct} /Ωcm^2	Z_W / $m\Omega$	^{2}
Pt	7.46 (3.43)	41.67 (3.19)	294.0 (3.83)	0.25 (17.39)	1.07×10^{-3}
Pt-MWCNT	7.91 (0.46)	70.00 (3.46)	3.07 (1.84)	0.48 (0.45)	1.94×10^{-5}
Pt-PB	7.52 (4.82)	40.67 (4.86)	185.7 (5.94)	0.14 (12.25)	9.54×10^{-5}
Pt-MWCNT-PB	9.23 (1.41)	375.67 (16.92)	2.66 (8.83)	1.42 (2.92)	2.40×10^{-4}

3.3. Electrocatalytic response of the analytes at the electrodes.

Previous studies have shown that iodate and periodate have better electrochemical activity in acidic medium and that this activity decreases with increasing pH [22,23], while sulphite electrocatalytic response was more favoured under alkaline pH conditions [24]. Effect of PB deposition time (2, 5, 10 and 15 min) was carried out and 5 min deposition time gave the optimum current response towards the analytes and was used through the study. Therefore, Figure 5a compares the current response of the Pt-MWCNT-PB modified electrode in both phosphate buffer alone and 8 mM IO_3^- solution. From this Figure, the reduction current due to the conversion of iodate ion to iodide, which was not found in the PBS electrolyte alone, confirmed clearly the catalytic activities of the Pt-MWCNT-PB electrode towards iodide reduction. In the same vein, the electrode also proved to be the best in the electrocatalytic reduction of iodate compared to other electrodes investigated (Fig. 5b). This is attributed to the presence of the MWCNT which increases the surface area of Pt-MWCNT-PB electrode thereby enhancing more PB particles deposition, and consequently creating more catalytic site for the electrocatalytic behaviour of the electrode towards the studied analytes compared with the other electrodes investigated. A similar trend was observed for electrocatalytic reduction of 8 mM periodate in pH 2.0 PBS (Fig. 5c) and electrocatalytic oxidation of 8 mM sulphite in 0.1 M NaOH electrolyte (Fig. 5d) on the studied electrodes. Contrary to the occurrence of iodate and periodate reduction current at the negative potential [25,26], their reduction current occurred at an unusual positive potential in this study, a phenomenon which was also observed by other workers for the analytes [23]. This is interesting, and an advantage to PB modified electrode towards reduction of iodate and periodate as it eliminates oxygen evolution process usually associated with reduction process at the negative potentials. In this work, the voltammetry data in terms of peak current and potential showed that the Pt-MWCNT-PB electrode demonstrated enhanced current response at a lower potential towards iodate and periodate reduction (mediated by the MWCNT-PB nanocomposite) and at lower starting potential of catalysis towards sulphite oxidation compared to the other electrodes. The results compared favourably with Salimi et al. [23] and Haghighi et al. works [22] where MWCNT have been implicated as mediating and enhancing the catalytic effect of the surface modifier on the electrode towards the analytes. The difference in their work and this study is the source (($FeCl_3$ and $K_3[Fe(CN)_6]$) of the PB catalyst used, which are common laboratory reagent, cheap, readily available and can be reduced to form PB on the Pt electrode using a simple electrodeposition technique. In all cases, the results indicate a strong catalytic effect of the Pt-MWCNT-PB nanocomposite modified electrode thus all further experiments were focussed on this electrode.
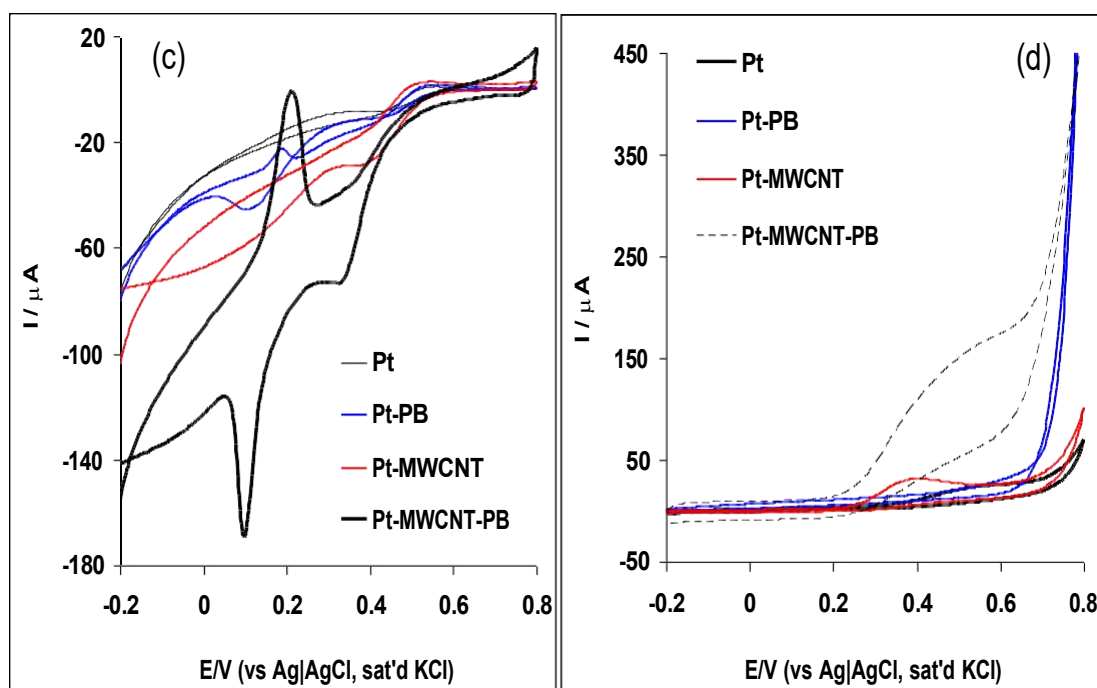
Figure 5. (a) Comparative current response of the modified Pt-MWCNT-PB electrode in pH 2.0 PBS alone, and pH 2.0 PBS + 8 mM IO_3^-. (b), (c) and (d) are the comparative cyclic voltammograms showing the current response of Pt, Pt-PB, Pt-MWCNT and Pt-MWCNT-PB modified electrodes in 8 mM IO_3^- in pH 2.0 PBS, 8 mM IO_4^- in pH 2.0 PBS and 8 mM SO_3^{2-} in 0.1 M NaOH respectively (Scan rate: 25 mVs^{-1}).

3.4. Stability and scan rate study

Pt-MWCNT-PB electrode was repetitively cycled in the analytes (20 scans) exemplified with iodate (Fig. 6a) and sulphite (Fig. 6b) to investigate the electrode stability or resistant to surface poison due to adsorbed species and reaction intermediates. A decrease in peak current was observed after the second and the first scan for iodate and sulphite respectively, which is typical of a poisoned electrode. Similar result was obtained for periodate. However, upon electrochemical cycling of the electrode in a fresh PBS (pH 7.0) solution, the electrode surface was renewed and a current recovery of *ca* 90% was obtained for iodate and periodate, and 125% recovery for sulphite. The results suggest stability and potential reusability of the electrode after successive experiment. To further probe the stability of the electrode, it was stored in a refrigerator for 15 days and re-used. No significant change in the initial current of the analytes was observed indicating the electrochemical stability and reproducibility of the catalyst on the electrode.
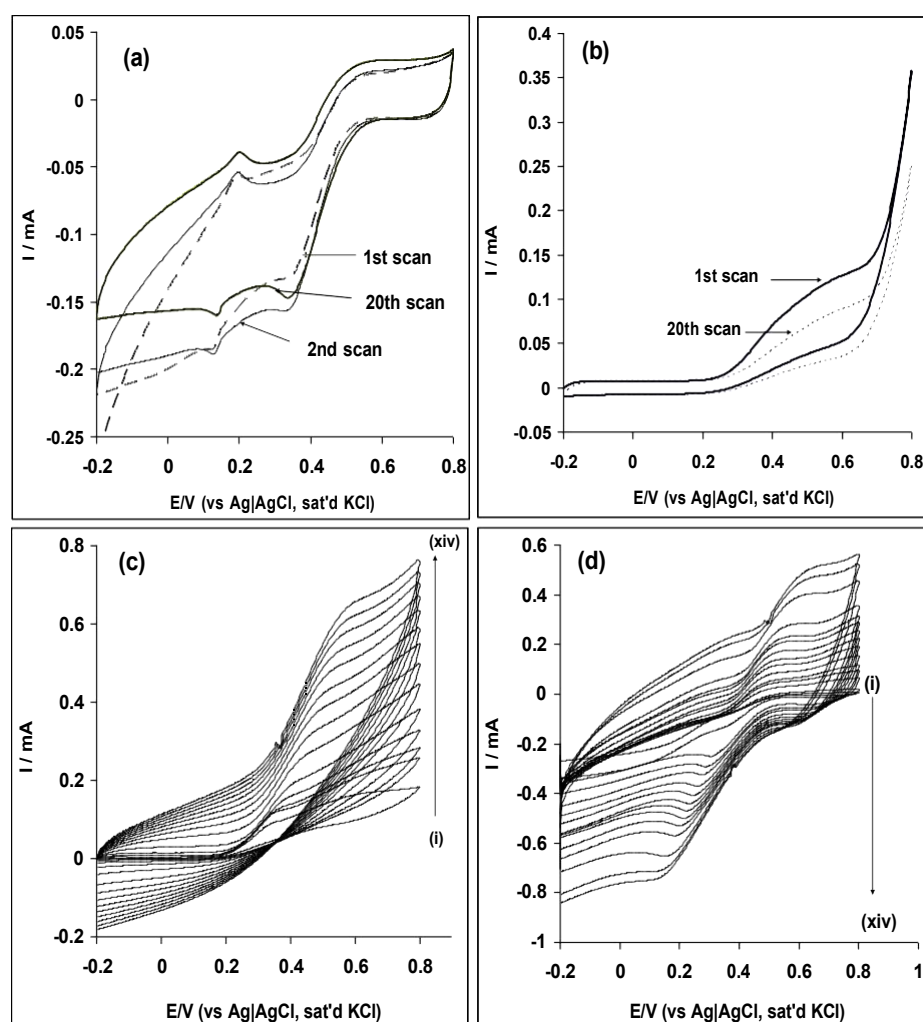
Figure 6. Repetitive cyclic voltammograms (20 cycles) of Pt-MWCNT-PB electrode in (a) 0.1 M PBS (pH 2.0) containing 8 mM IO_3^- and (b) 0.1 M NaOH containing 8 mM SO_3^{2-} (scan rate: 25mVs^{-1}). (c) Current response of the Pt-MWCNT-PB electrode in 8 mM SO_3^{2-} solution (scan rate: 25-1000 mVs^{-1}, inner to outer) and (d) Current response of the Pt-MWCNT-PB electrode in 8 mM IO_4^- solution (scan rate: 25-1000 mVs^{-1}, inner to outer).

The effect of scan rate (   ) (scan rate: 25-1000 mVs^{-1}) on the electrocatalytic oxidation and reduction of the analytes was investigated and the voltammograms obtained are exemplified with sulphite and periodate (Fig. 6c and 6d). In all cases, the reduction peak potential for iodate and periodate shifted slightly negatively, while the oxidation peak potential for sulphite shifted slightly positively with increasing scan rates. The current function plots (Ip/v$^{1/2}$ vs v) obtained for the analytes (Fig. 7a) gave the characteristic curves confirming the interplay of coupled electrochemical-chemical (EC$_{cat}$) reaction processes at the electrode. Similarly, the plots of log I_p vs log v (Fig. 7b) are linear with slopes values lower than the 0.5 expected for an ideal diffusion-controlled process [44,45], therefore, suggesting the possibility of the involvement of an adsorbed reaction intermediates.
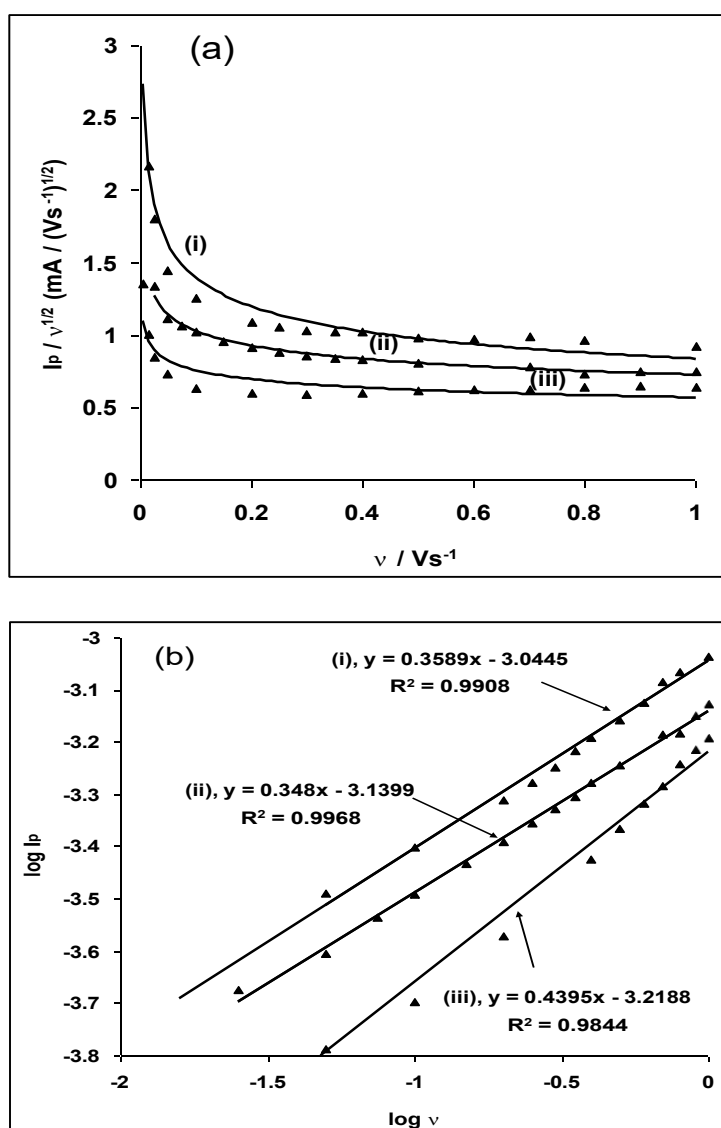
Figure 7. (a) Current function plots of (I_p/   vs   ) for (i) IO$_3^-$, (ii) IO$_4^-$ and (iii) SO$_3^{2-}$. (b) Plots of log I_p vs log   for (i) IO$_3^-$, (ii) IO$_4^-$ and (iii) SO$_3^{2-}$.

From the Tafel equation (Eqn.3) for a totally irreversible diffusion- controlled process [42],

$$E_p \quad constant \quad - \quad \frac{b}{2} \quad log \quad \quad\quad\quad (3)$$

plots of E_p versus log υ gave a linear relationship (not shown) and the slope ($\partial E_p / \partial (\log v)$) of this plot also known as Tafel slope b was obtained for iodate, periodate and sulphite respectively. The values of b are presented in Table 2.0. These values are higher than the theoretical 118 mV dec^{-1} for a one-electron process involved in the rate-determining step. Therefore, such high Tafel values are attributed to the adsorption of reactants or intermediates on the electrode surfaces and/or reactions occurring within a porous electrode structure [46].

Table 2. Electrocatalytic parameters obtained for the analytes on the Pt-MWCNT-PB modified electrode.

Analyte	Electrocatalytic parameters					
	Sensitivity ($\mu A/\mu M$)	LCR (μM)	LoD (μM)	Tafel slope(b) (mV dec^{-1})	$10^{-6}k_{cat}$ (cm^{3}mol^{-1}s^{-1})	10^5D /cm^{2}s^{-1}
Iodate	0.021	34.0-268.3	8.30±0.92	211.0	1.37±0.05	8.11±0.48
Periodate	0.025	16.4-142.9	8.06±0.52	176.2	0.34±0.01	4.49±0.13
Sulphite	0.127	16.4-142.9	4.70±0.14	129.2	52.4±0.5	1.42±0.13

3.5. Amperometric detection of the analytes
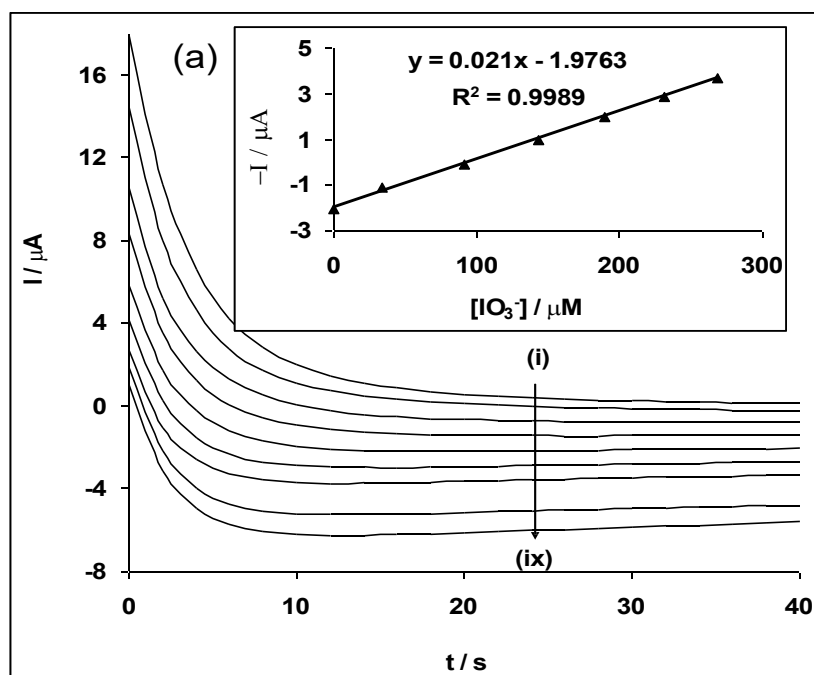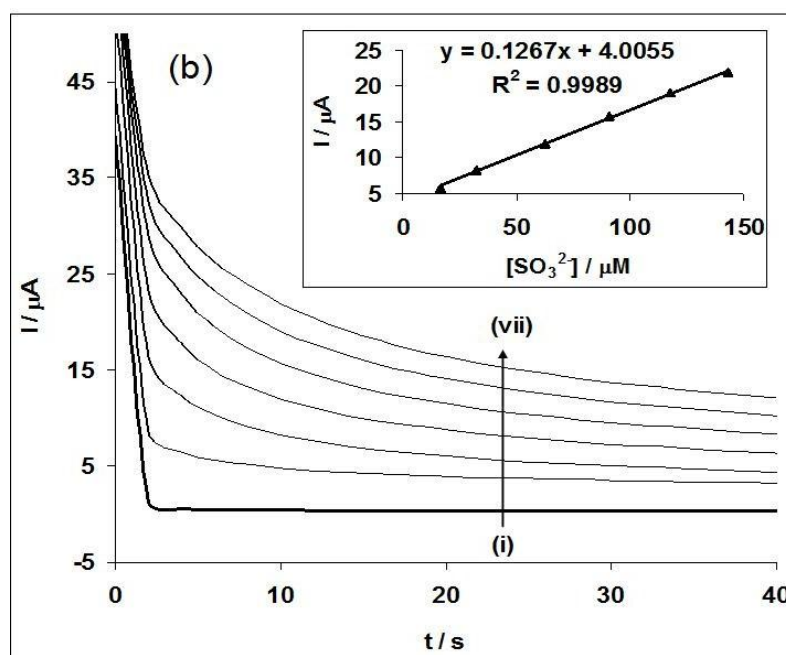
Figure 8. Typical chronoamperogram of Pt-MWCNT-PB in (a) pH 2.0 PBS containing different concentrations of IO_3^- (0.0, 34.0, 90.9, 142.9, 189.2, 230.8, 268.3, 333.3, and 375.0 µM (i - ix)), (b) 0.1 M NaOH containing different concentrations of SO_3^{2-} (0.0, 16.4, 32.3, 62.5, 90.9, 117.7 and 142.9 µM (i - vii)). Inset in (a) and (b) are the linear plots obtained from current response vs IO_3^- and SO_3^{2-} concentration respectively.

Amperometric detection of iodate, periodate and sulphite on Pt-MWCNT-PB electrode was carried out during successive addition of the different concentrations of the analytes in their respective electrolytes, and at a fixed potential of 0.32 V for iodate and periodate, and 0.6 V for sulphite The chronoamperogramms obtained are represented with iodate and sulphite in Figure 8. The insets depict the calibration curve for the plot of current against concentration.

The limit of detection (LoD) was calculated based on the relationship [47]:

$$LoD \quad \frac{3.3}{m}$$

(4)

where δ is the relative standard deviation of the intercept of the y-coordinates from the line of best fit, and m the slope of the same line. The sensitivity, linear concentrations range (LCR) and limit of detection (LoD) are also summarised in Table 2.0. The detection limits obtained for iodate and periodate in this study compared favourably with 15 µM reported for iodate on GCE/MWCNTs/[C_8Py][PF_6]-PMo_{12} [22], 2.5 µM for iodate on MWCNT-iron-porphyrins-GC electrode [23], and 0.5 µM for periodate at V-Schiff base complex/MWCNTs modified GC electrode [48]. On the other hand, the limit of detection obtained for sulphite agreed closely with 3.0 µM and 1.9 µM reported for the analyte on nickel powder carbon composite modified electrode [49] and nickel pentacyanonitrosylferrate(NiPCNF) film modified/Al electrode [50] respectively but much lower compared to 80 µM reported for the analyte on Prussian blue modified glassy carbon electrode [51] .

The micro molar detection limit obtained for the analytes in this work was low enough for their trace determination in real life samples.

From the concentrations study, the diffusion coefficient D for the analytes and the catalytic rate constant K for the Pt-MWCNT-PB electrode was estimated by using Equations 5 [38] and 6 [52]:

$$\frac{I}{2C} = \frac{nFAD}{\pi^{1/2}t^{1/2}} \tag{5}$$

$$\frac{I_{cat}}{I_L} = \pi^{1/2}\,k_{cat}^{1/2}\,C_o^{1/2}\,t^{1/2} \tag{6}$$

where C is the bulk concentration (molcm^{-3}), A is the area of the electrode in cm^2, n is the number of electrons which is approximately 6 for iodate and periodate [53], I_{cat} and I_L are the currents in the presence and absence of the analyte. From the experimental plots of I versus $t^{-1/2}$, the diffusion coefficient D of the analytes was calculated and reported in Table 2.0. Similarly, from the plot of I_{cat}/I_L vs $t^{1/2}$, the k_{cat} for Pt-MWCNT-PB in the analytes were obtained (Table 2.0). The D values obtained in this study for iodate and periodate are within the same magnitude with 4.5 and 5.6 x 10^{-5} cm^{2}s^{-1} reported for iodate and periodate [23].
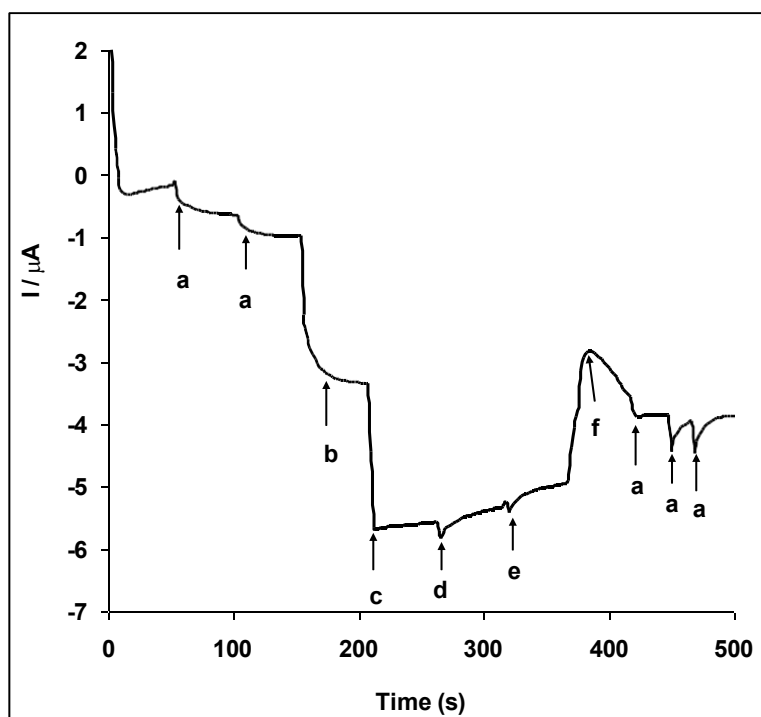

Figure 9. Typical Amperometric response of Pt-MWCNT-PB electrode for (a) 1.8 mM IO$_3^-$ and in the presence of 1.0 mM of various interference species (b) nitric oxide (NO), (c) nitrite (NO$_2^-$), (d) bromate (BrO$_3^-$), (e) chlorate (ClO$_3^-$) and (f) sulphite (SO$_3^{2-}$). A potential of 0.32 V and PBS of pH 2 was used.

The K_{cat} value of 5240 x 10^4 cm^{3}mol^{-1}s^{-1} obtained for sulphite in this study is a magnitude higher than 3600 x 10^3 cm^{3}mol^{-1}s^{-1} reported for the analyte and other sulphur oxoanions on nickel oxide film modified carbon composite electrode [50]. The difference in the magnitude of K was attributed to the different catalyst or electrode modifier, and their extent of interaction with sulphite molecules. The K_{cat} values of 1.37 and 0.34 x 10^6 cm^{3}mol^{-1}s^{-1} obtained for iodate and periodate respectively were lower compared to 8.4 and 8.83 x 10^6 cm^{3}mol^{-1}s^{-1} reported for the analytes on V-Schiff base complex/MWCNTs modified GC electrode [48]. The high K_{cat} (10^6-10^7 cm^{3}mol^{-1}s^{-1}) values obtained in this study indicate excellent activity of the MWCNT/PB film towards iodate and periodate reduction and sulphite oxidation.

3.6. Amperometric determination of iodate in the presence of other interfering species.

Amperometric responses of IO_3^- in the presence of other interfering ions are shown in Figure 9. Iodate reduction current was determined before and after 400 seconds of injection of other interfering species. The results presented in Figure 9 therefore showed that there was no interfering effect to iodate current after the addition of these other species.

3.7. Real sample analysis: Determination of iodine content of iodated table salts
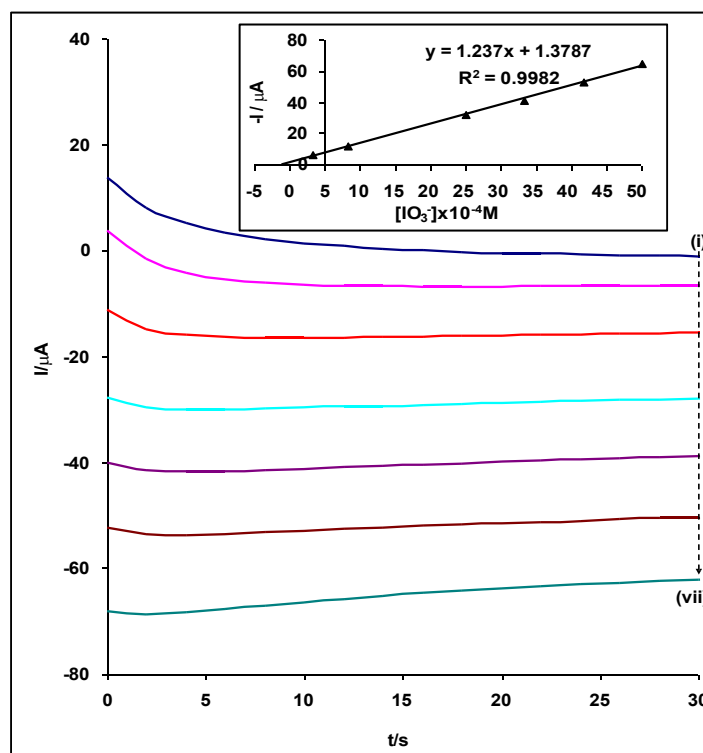
Figure 10. Typical chronoamperogram of Pt-MWCNT-PB in pH 2.0 PBS containing commercial table salt spiked with different concentration of standard iodate (IO_3^-) solution (0.00, 0.33, 0.83, 2.50, 3.33, 4.17and 5.00 mM (i - vii)) (standard addition method). Inset is the linear plots obtained from current response vs IO_3^- concentration.

The potential application of the fabricated sensor was tested by determining the iodine content of iodated table salts. The procedure for the iodine content determination was already discussed under experimental. The chronoamperograms obtained for both spiked and unspiked samples is presented in Figure 10, while inset in Figure 10 presents the plot of iodate reduction current against concentrations. The experiment was repeated five times (n=5) for every salt sample analyzed. The iodate content of the salt (in terms of iodine) was determined by extrapolation (See inset in Figure 10). Assuming a set standard of 70 µg/g of iodine supplement in table salt [54], the concentration found in each table salt (n=5) (Table 3) is approximately within this set standard. The result clearly indicates the suitability of the fabricated sensor for iodine level determination in iodated table salts.

Table 3. Determination of iodine content of commercially available iodated table salts (n =5)

Sample	Concentration found (μg/g)	Recovery (%)
1	73.5 ± 5.0	105.0 ± 7.1
2	76.0 ± 5.8	108.6 ± 8.2
3	78.5 ± 5.0	112.1 ± 7.1

3. CONCLUSIONS

This work describes the electron transfer and electrocatalytic behaviour of multi-walled carbon nanotubes Prussian blue modified platinum electrode. The Pt-MWCNT-PB electrode demonstrated fast electron transfer kinetics and enhanced electrocatalytic response towards the studied analytes compared to other electrodes investigated. Reduction of iodate and periodate occurred at unusual positive potential, which is good in eliminating interference due to oxygen evolution at the negative potential. The catalytic process was associated with adsorbed oxidation/reduction intermediates. The Pt-MWCNT-PB electrode can conveniently detect iodate in the presence of other interfering species, and can be used for the determination of iodine content of commercially available iodated table salts.

References

J. Hazard Mat., 123 (2005) 250, A. Afkhami, T. Madrakian, and M. Bahram.

In their 2006 publication "Electroanalysis," M.A. Rahman, M.-S. Won, P.-H. Wei, and Y.-B. Shim present their findings.

Thirdly, in Electroanalysis, 20 (2008) 1873, A. Balamurugan and S.-M. Chen collaborate.

In Electroanalysis, 22 (2010) 1812, R. Thangamamuthu, Y.-C. Pan, and S.-M. Chen wrote the article.

The following sources were cited: 5. A. Salimi, R. Hallaj, B. Kavosi, B. Hagighi, Anal. Chim. Acta, 661 (2010) 28; 6. D. Pearson, The Chemical Analysis of Foods, Churchill Livingstone: Edinburgh, London and New York, 1976; pp. 29; 7. K. Finster, J. Sulfur Chem., 29 (2008) 281; 8. J.G. Muller, R.P. Hickerson, R.J. Perez, C. Burrows, J. Am. Chem. Soc., 119, (1997) 1501.

9.Z. Meng, N. Sang, B. Zhang, Bull. Environ. Contam. Toxicol., 69 (2002) 257. 10.G. Selvarani, S.K. Prashant, A.K. Sahu, P. Sridhar, S. Pitchumani, A.K. Shukla, J. Power Sources, 17 (2008) 86. 11.K.C. Pan, C.S. Chuang, S.H. Cheng, Y.O. Su, J. Electroanal. Chem., 501 (2001)160. 12.D. Moscone, D. D'Ottavi, D. Compagnone, G. Palleschi, A. Amine, Anal. Chem., 73 (2001) 2529. 13.K. Zhao, H. Song, S. Zhung, L. Dai, P. He, Y Fang, Electrochem. Commun., 9 (2007) 65. 14.F. Qu, A. Shi, M. Yang, J. Jiang, G. Shen, R. Yu, Anal. Chimic. Acta, 605 (2007) 28. 15.S. Han, Y. Chen, R. Pang, P. Wan, Ind. Eng. Chem. Res., 46 (2007) 6847. 16.Y. Shan, G. Yang, J. Gong, X. Zhang, L. Zhu, L. Qu, Electrochim. Acta,

53, (2008) 7751. 17.Y. Xian, Y. Zhoua, Y. Xian, L. Zhouc, H. Wang, L. Jin, Anal. Chimic.Acta Y. Miao, J. Chen, X. Wu, J Miao, Physicochem. Eng. Aspects, 295 (2007) 135. 19.A-M. Gurban, T. Noguer, C. Bala, L. Rotariu, Sens. Actuat. B, 128 (2008) 536. 20.X. Huang, Y. Li, Y. Chen, L. Wang, Sens. Actuat. B, 134 (2008) 780. 21.D. Sun, L. Zhu, H. Huang, G. Zhu, J. Electroanal. Chem., 597 (2006) 39. 22.B. Haghighi, H. Hamidi, L. Gorton, Electrochim. Acta, 55 (2010) 4750. 23.A. Salimi, A. Noorbakhsh, M. Ghadermarzi, Sens. Actuat. B, 123 (2007) 530. 24.J.R.C. Rocha, T.L. Ferreira, R.M. Torresi, M. Bertotti, Talanta, 69 (2006) 148. 25.O. Ordeig, C.E. Banks, F.J.D. Campo, F.X. Munoz, R.G. Compton, Electroanalysis, 18 (2006) 1672. 26.A. Salimi, M. Roushani, R. Hallaj, Electrochim. Acta, 51 (2006) 1952. 27.T.R.L. Dadamos, M.F.S. Teixeira, Electrochim. Acta, 54 (2009) 4552. 28.T. Yama Scientific American, 356 (1997) 85. 30 (written by M.S. El-Shahawi). In their publication titled "Anal. Chim. Acta," Decnop-Weever and Kraak (1997) p. 125. 31. Reference: J. Analytical Chemistry, 345 (1980) 733, by Y.M. Temerk, M.E. Ahmed, and M.M. Kamal. The authors of the following publications: - Journal of Power Sources, 191 (2009) 366; - Colloids and Surfaces B: Biointerfaces, 84 (2011) 454; - J. Electroanal. Chem., 97 (1998) 456; - X. Che, R. Yuan, Y. Chai, J. Li, Z. Song, W. Li, X. Zhong. In an article published in 2005 by Electrochem. Commun., Y-L. Hu, J-H. Yuan, W. Chen, K. Wang, and X-H. Xia discuss various topics. In a 2007 article for Bioelectrochemistry, A. Ernst cites research by K. Itaya, N. Shoji, and I. Uchida. In an article published in 1984 by the Journal of the American Chemical Society, K. Itaya cites research by K. Itaya, N. Shoji, and I. Uchida. Finally, in an article published in 2000 by John Wiley & Sons Inc., J. Wang explains the fundamentals of analytical electrochemistry.
39.G. Sánchez-Pomales, L. Santiago-Rodríguez, N.E. Rivera-Vélez, C.R. Cabrera, J. Electroanal. Chem., 611 (2007) 80. 40.R. Raghavendra Naik, E. Niranjana, B. E. Kumara Swamy, B. S. Sherigara, H. Jayadevappa, Int. J. Electrochem. Sci., 3 (2008) 1574. 41.D. Nkosi, K.I. Ozoemena, J. Electroanal. Chem., 621 (2008) 304. 42.M.E. Orazem, B. Tribollet, Electrochemical Impedance Spectroscopy, John Wiley & Sons, Inc.: New Jersey, 2008
Int. J. Electrochem. Sci., 6 (2011) 673, O.A. Arotiba, P.G. Baker, B.B. Mamba, and E.I. Iwuoha reported this in their work. A.S. Kumar, P.-Y. Chen, J.-M. Zen, Y. Shih, and Talanta, 62 (2004) 912. 45. A.S. Kumar, J.-C. Chen, and J.-M. Zen, "Anal. Chem., 73 (2001) 1169." 46. Publication: J. Phys. Chem. B., 110 (2006) 10401, by J.N. Soderberg, A.C. Co, A.H.C. Sirk, and V.I. Birss.

Analytical Chemistry, 6th edition, by Christian G. D., Wiley: New York, 2004, pp. 113–48. The following references are cited: 1. A. Salimi, H. Mamkhezri, S. Electrochem. Commun., 8 (2006) 688. 2. M.H. Pournaghi-Azar, M. Hydarpour, H. Dastangoo, Anal. Chim. Acta, 497 (2003) 133. 3. Salimi, A., M. Roushani, R. Hallaj, Electrochem. Acta, 51 (2006) 1952. 4. Garcia, E., Lorenzo, F., Sens. Actuat. B, 106 (2005) 803. 52. In their 2006 article, K.M. Manesh, P. Santosh, A.I. Gopalan, and K.P. Lee published in Electroanalysis, 53.A. Salimi, H. Mamkhezri, R. Hallaj, and S. Zandi appeared in Electrochim. Acta, 52 (2007), page 6097. In their 2007 article, 54.S.L. Lee, S. Ananthakrishnan, E.N. Pearce, et al. contributed to Medscape Drugs, Conditions and Procedures. (20 March 2012, last updated online)